Human Molecular Genetics, 2022, Vol. 31, No. 2 157–165

https://doi.org/10.1093/hmg/ddab217
Advance Access Publication Date: 26 July 2021
General Article

GENERAL ARTICLE

Common variants in *SCN10A* gene associated with Brugada syndrome

Yan Huang[1,2,‡], Xiao-Meng Chen[3,‡], Hector Barajas-Martinez[4], Hong Jiang[1,2], Charles Antzelevitch[4] and Dan Hu[1,2,*,†]

[1]Department of Cardiology and Cardiovascular Research Institute, Renmin Hospital of Wuhan University, Wuhan, Hubei 430060, China, [2]Hubei Key Laboratory of Cardiology, Wuhan, Hubei 430060, China, [3]Department of Cardiology, Qingdao Municipal Hospital, School of Medicine, Qingdao University, Qingdao 266071, China and [4]Lankenau Institute for Medical Research, and Lankenau Heart Institute, Wynnwood, Pennsylvania and Jefferson Medical College, Philadelphia, PA 19096, USA

*To whom correspondence should be addressed at: Department of Cardiology and Cardiovascular Research Institute, Renmin Hospital of Wuhan University, 238 Jiefang Road, Wuhan 430060, China. Tel: +86-27-88041911; Fax: +86-27-88042292; Email: hudan0716@hotmail.com; rm002646@whu.edu.cn

Abstract

Genome-wide association studies indicate that *SCN10A* plays an important role in cardiac electrophysiology. Common and rare *SCN10A* variants are suggested to contribute to Brugada Syndrome (BrS), an inherited channelopathy resulting from genetic-determined loss-of-function in cardiac sodium channel. This study sought to characterize the role of *SCN10A* common variants in BrS. Clinical and genetic analyses were performed in 197 patients diagnosed with BrS. Baseline ECG parameters were evaluated in patients carrying each of four common variants associated with BrS. Cellular electrophysiological study was performed in *SCN5A-SCN10A* co-transfected TSA201 cells to investigate the possible electrophysiological characteristics of the allele of rs6795970, which displayed the most significant association with BrS. Four *SCN10A* common variants (rs7630989, rs57326399, rs6795970, rs12632942) displayed significant association with BrS susceptibility. There were no evident associations between baseline ECG parameters in BrS patients and the different genotypes of the four variants. Rs6795970 (V1073) was strongly associated with a risk for BrS, which suggests the different electrophysiological characters between these two alleles. Functional study showed a positive shift in steady-state activation ($V_{1/2}$: -62.2 ± 2.6 *vs.* -53.5 ± 1.6 for A1073 and V1073 group, respectively; $P < 0.05$) and slower recovery from inactivation in mutant *SCN5A-SCN10A* co-transfected cells with, which contribute to the slow conduction in BrS patients with rs6795970. In conclusion, *SCN10A* common variants are associated with increased susceptibility to BrS. An allele rs6795970 (V1073) increases the risk for BrS. The electrophysiological changes in a positive shift in steady-state activation and slower recovery from inactivation by *SCN10A*-V1073 contribute to this variant associated BrS.

†Dan Hu, http://orcid.org/0000-0002-0994-8434
‡Both contributed equally as the first authors.
Received: June 29, 2021. **Revised:** July 19, 2021. **Accepted:** July 20, 2021

Introduction

Brugada syndrome (BrS) is an inherited cardiac arrhythmia associated with ST-segment elevation in the right precordial leads (V1–V3) of electrocardiogram (ECG) and a predisposition to sudden cardiac death (SCD) secondary to the development of ventricular fibrillation (VF) (1,2). Although around 20 mutations have been associated with BrS, nearly two thirds of BrS patients remain genetically undetermined. Mutations in the *SCN5A* gene which encodes the α-subunit of the canonical cardiac sodium channel Nav1.5, account for approximately 20% in the genotyped BrS cases (3).

Nav 1.8, encoded by *SCN10A*, is a neuronal sodium channel first identified in small sensory neurons of dorsal root ganglion. Since 2010, consecutive genome-wide association studies (GWAS) have highlighted association of the *SCN5A–SCN10A* locus with a variety of electrocardiographic parameters and arrhythmic manifestation (4–6). Common variants in *SCN10A* (rs6795970, rs6800541, rs6801957) have been identified as significantly associated with the PR interval and (or) QRS duration, which reflect the process of cardiac conduction and ventricular depolarization (7,8). Thus, the role of $Na_v1.8$ in cardiac electrophysiology has been of increasing interest.

One recent GWAS reported that a common variant (rs10428132) in *SCN10A* is significantly associated with susceptibility to BrS (9). An earlier study by our group revealed rare *SCN10A* variants carried by BrS patients. These genetic defects caused a loss-of-function of sodium channel when the mutant plasmids were expressed *ex vivo* (10). Other variants including W189R, R844H, N1328K, R1380Q and R1863Q were also reported to be associated with BrS (11,12). It is noteworthy that very low levels of $Na_v1.8$ mRNA can be detected in ventricular tissue (13–15). One hypothesis suggested that *SCN10A* may affect cardiac electrophysiology via regulation of *SCN5A* expression or channel properties (10,16,17). In the present study, we evaluated 197 BrS cases referred to Renmin hospital of Wuhan University between 2008 and 2018 with respect to an association between *SCN10A* variants and ECG parameters, including heart rate (HR), PR interval, QRS duration and QTc interval. Additionally, we investigated the possible electrophysiological consequences of the common variant rs6795970 when *SCN10A* and *SCN5A* plasmids were co-expressed in mammalian cells *ex vivo*.

Results

Study population

A total of 197 unrelated BrS patients were included in this study. The baseline clinical profile is presented in Table 1. A majority of patients were male (64.0%) with a mean age of 45.0 ± 16.0 years at time of diagnosis. Sixty-seven patients (34.0%) displayed a spontaneous type-1 ECG, and 21 (10.7%) had a family history of SCD. Patients presenting with syncope and those with aborted SCD or SCD comprised 22.8% and 14.2% of the cohort, respectively. Twenty-seven (13.7%) patients had a history of ventricular tachycardia or VF. Atrial fibrillation (AF) was recorded in 11 patients (5.6%). Twenty-six (13.2%) presented with cardiac conduction defect (CCD) and 22 (11.2%) with early repolarization syndrome (ERS).

Table 1. Clinical profile of enrolled patients

Parameters	Value (Percentage)
Age (yrs)	45 ± 16
Male	126 (64.0%)
Spontaneous Type I ECG	67 (34.0%)
Family history of SCD	21 (10.7%)
Asymptom	76 (38.6%)
Symptoms	
Syncope	45 (22.8%)
SCD/ASCD	28 (14.2%)
Documented VT/VF	27 (13.7%)
AF	11 (5.6%)
CCD	26 (13.2%)
ERS	22 (11.2%)

Age presents as mean ± SD; N = 197.

Common variant analysis

Four non-synonymous common variants (MAF > 0.01) in *SCN10A* were identified in the 197 unrelated BrS patients (Table 2). All were located in the cytoplasmic domain between IIS6-IIIS1. Our patients were of European, African and Asian descent. Genotype frequencies from ESP (European American and African American), 1000 genomes and gnomAD are presented in Table 2, showing minor and major allele distribution in the BrS cases as well as controls from ESP, 1000 genomes and gnomAD databases. All of the screened common variants were significantly associated with BrS compared to the controls (S509P/rs7630989, I962V/rs57326399, A1073V/rs6795970, L1092P/rs12632942). As shown in Table 3, the minor allele, in rs7630989, rs57326399 and rs12632942, has a protective influence on the susceptibility to BrS when compared to the data from Exome Sequencing Project (ESP), 1000 genomes and gnomAD, respectively. For the rs6795970, the minor allele 'A', encoding amino-acid 'V', is strongly associated with the risk of BrS (OR = 3.0, $P = 5.161 \times 10^{-28}$ versus ESP; OR = 4.0, $P = 4.483 \times 10^{-42}$ versus 1000 genomes; OR = 2.4, $P = 3.451 \times 10^{-19}$ versus gnomAD). In contrast to the controls, more BrS patients carried A allele (V1073) at this locus (MAF: 0.56 in BrS versus 0.30 in ESP, $P = 5.161 \times 10^{-28}$; 0.56 in BrS versus 0.24 in 1000 genomes, $P = 4.483 \times 10^{-42}$; 0.556 in BrS versus 0.342 in gnomAD, $P = 3.451 \times 10^{-19}$).

ECG analysis

Baseline ECG parameters including HR, PR interval, QRS duration and QTc interval were calculated in patients to characterize the variance among the four different genotypes. Table 4 summarizes the ECG parameters measured from the three genotypes of rs6795970-GG, AG and AA. No significant difference was found in the compared parameters except for QTc interval in lead V2 before, but not after adjusting for age and gender. The measurement of these parameters among the other three variants (rs7630989, rs57326399, rs12632942) is displayed in Tables 5–7. No difference was observed among the different genotypes of the three protective variants.

Functional studies

To further assess the electrophysiological characteristics of the most significant non-synonymous variant-A1073V, we performed patch-clamp studies in *SCN5A–SCN3B–SCN10A* co-expressed TSA201 cells. The ion currents in WT and the variant co-transfected cells showed a similar reversal potential ($+43.3 \pm 4.0$ mV). V1073 co-transfected cells were also sensitive to the selective Nav1.8 inhibitor (A-803467). Representative traces of *SCN5A–SCN3B–SCN10A* (A1073, G allele of rs6795970)

Table 2. Common variants in *SCN10A* in BrS patients

SCN10A Variant	SNP ID	Location	Minor/Major alleles	Genotype distribution											
				BrS cases			ESP (EA + AA)			1000 Genomes			GnomAD		
				Hom (minor)	Het	Hom (major)	Hom (minor)	Het	Hom (major)	Hom (minor)	Het	Hom (major)	Hom (minor)	Het	Hom (major)
S509P	rs7630989	Exon11; IS6-IIS1	G/A	0	14	183	114	138	5451	80	541	1883	1434	18 038	120 614
I962V	rs57326399	Exon16; IIS6-IIIS1	C/T	2	52	143	320	2095	4088	140	775	1598	8736	49 139	83 305
A1073V	rs6795970	Exon18; IIS6-IIIS1	A/G	65	89	43	700	2469	3334	298	820	1488	80 356	59 408	62 301
L1092P	rs12632942	Exon18; IIS6-IIIS1	G/A	0	49	148	335	2191	3977	144	812	1548	8504	48 866	80 259

and *SCN5A–SCN3B–SCN10A* (V1073, A allele of rs6795970) were displayed in Figure 1A. No significant difference was observed in the I–V relationship between the WT and mutant channels ($I_{Na,P}$ at −40 mV in A1073: −486.9 ± 71.8 pA/pF, n = 29; $I_{Na,P}$ at −30 mV in V1073: −390.3 ± 72.4 pA/pF, $n = 29$; $P = 0.347$, Fig. 1B). To compare the blocking effect of 100 nM A-803467 on A1073 and V1073 transfected cells, relative current was evaluated before and after the drug. There was no obvious difference in $I_{Na,P}$ reduction between the two alleles after the transfected cells were exposed to the drug. In Figure 1C, the current reduced to 64.5 ± 6.7% in A1073 transfected cells and 59.2 ± 3.6% in V1073 ($P < 0.01$, $n = 13$ in A1073; $P < 0.01$, $n = 15$ in V1073; $P = 0.449$ in A1073 versus V1073 on the current decrease after the drug). The significant positive shift of steady-state activation was noted in V1073 ($V_{1/2}$: A1073 = –62.2 ± 2.6 mV, V1073 = –53.5 ± 1.6 mV, $P = 0.006$, K: A1073 = 5.1 ± 0.3 mV, V1073 = 4.2 ± 0.4 mV, $P = 0.092$, Fig. 1D). V1073 exhibited a higher activation threshold than A1073, which suggested a loss of function of sodium channel, may contribute to a much slower-conduction substrate when BrS patients carrying A allele (V1073). After applying A-803467, the steady-state activation voltage was negatively shifted, but statistical difference was only observed in V1073 group ($V_{1/2}$: V1073 before the drug = −53.5 ± 1.6 mV, V1073 after the drug = −57.7 ± 1.9 mV, $P = 0.012$, Table 8).

Steady-state inactivation was then analyzed in A1073 and V1073 transfected cells in the absence and presence of A-803467. As shown in Figure 1E and Table 8, $V_{1/2}$ in both A1073 and V1073 transfected cells was negatively shifted about 10 mV after the drug was administrated ($V_{1/2}$: A1073 versus A1073 + Drug, $P < 0.001$; V1073 versus V1073 + Drug, $P < 0.001$; A1073 versus V1073, $P = 0.377$; A1073 + Drug versus V1073 + Drug, $P = 0.482$). In addition, kinetics of recovery from inactivation was also summarized in the two kinds of transfected cells before and after A-803467 (Fig. 2A and B and Table 8). The whole recovery process from inactivation after applying the drug became much slower in both A1073 and V1073 transfected cells in comparison to that before the drug (τ_{fast}: V1073 versus V1073 + Drug, $P = 0.006$; A1073 versus A1073 + Drug, $P = 0.002$; τ_{slow}: V1073 versus V1073 + Drug, $P = 0.014$; A1073 versus A1073 + Drug, $P = 0.044$; Table 8). Another prominent difference was displayed in the slow phase recovery process between A1073 and V1073 transfected cells in the absence of drug. Relative to that in A1073 cells, the slow recovery phase was prolonged in V1073 cells (τ_{slow}: A1073 versus V1073, $P = 0.029$, Table 8). Probably owing to the slower recovery in V1073 transfected cells, current block in V1073 appeared to be more than that in A1073 after 40 pulses at 10 Hz pacing (Fig. 2C and D). Besides, similar use-dependent block effects of A-803467 were found in A1073 and V1073 during 1 or 10 Hz pacing.

Discussion

The present study included 197 unrelated BrS patients in whom four non-synonymous common variants were identified—rs57326399, rs7630989, rs6795970 and rs12632942, which were revealed to have a significant association to BrS susceptibility. However, no significant associations were observed between the genotypes of the four variants and the baseline ECG parameters of the BrS patients enrolled. A allele in rs6795970 (V1073) has a significant predisposition to the risk of BrS and patients who carried 'V1073' tended to have a slower HR, wider QRS duration and shorter QTc interval compared with 'A1073' (G allele). Cellular electrophysiological studies in *SCN5A–SCN3B–SCN10A* co-expressed cells demonstrated that V1073 exhibits a more depolarized steady-state activation and a slowing of

Table 3. The risk of common variants in *SCN10A* to BrS

SCN10A Variant	SNP ID	Minor allele frequency									
		Cases	ESP	*P* value	Odds ratio (95% CI)	1000 Genomes	*P* value	Odds ratio (95% CI)	GnomAD	*P* value	Odds ratio (95% CI)
S509P	rs7630989	0.036	0.090	1.881E-4	0.374(0.219–0.640)	0.140	3.855E-9	0.226 (0.132–0.388)	0.075	0.003	0.457 (0.268–0.779)
I962V	rs57326399	0.142	0.210	0.001	0.622 (0.467–0.828)	0.211	0.001	0.621 (0.464–0.830)	0.236	1.200E-5	0.537 (0.404–0.712)
A1073V	**rs6795970**	**0.556**	**0.297**	**5.161E-28**	**2.955 (2.414–3.618)**	**0.242**	**4.483E-42**	**3.919 (3.180–4.830)**	**0.342**	**3.451E-19**	**2.411 (1.976–2.941)**
L1092P	rs12632942	0.124	0.220	3.894E-6	0.498 (0.368–0.673)	0.220	8.000E-6	0.503 (0.370–0.684)	0.239	9.030E-8	0.451 (0.335–0.609)

Note: The bold represents the SNP with the increased risk of BrS.

Table 4. Baseline ECG characterization of rs6795970 in BrS patients

Parameters	GG	AG	AA	*P* value
Heart rate (bpm)	78.000 ± 12.556	73.584 ± 12.984	74.511 ± 12.663	0.301
PR II (ms)	164.354 ± 24.622	165.443 ± 29.071	165.409 ± 21.605	0.981
PR V2 (ms)	162.261 ± 23.071	160.513 ± 30.015	161.763 ± 22.575	0.947
QRS II (ms)	96.905 ± 12.733	98.476 ± 13.658	101.351 ± 11.725	0.313
QRS V2 (ms)	100.025 ± 14.227	99.861 ± 13.392	101.426 ± 11.021	0.809
QTc II (ms)	413.582 ± 30.156	402.390 ± 32.004	404.547 ± 31.646	0.309
QTc V2 (ms)	417.102 ± 30.342	398.574 ± 32.950	400.697 ± 31.631	0.041*,**

Note: The value presents as Mean ± SD.
*$P < 0.05$: Baseline QTc interval at lead V2 in genotype AA versus AV.
**$P = 0.700$ after adjusted by age and gender.

Table 5. Baseline ECG characterization of rs7630989 in BrS patients

Parameters	GG	AG	*P* value
Heart rate (bpm)	74.795 ± 13.193	74.917 ± 8.106	0.799
PR II (ms)	165.478 ± 26.407	162.146 ± 16.373	0.892
PR V2 (ms)	161.166 ± 27.059	162.598 ± 15.076	0.685
QRS II (ms)	99.025 ± 13.328	100.102 ± 5.694	0.782
QRS V2 (ms)	100.601 ± 13.056	98.078 ± 9.197	0.647
QTc II (ms)	406.294 ± 31.800	397.846 ± 29.062	0.519
QTc V2 (ms)	405.074 ± 32.768	395.129 ± 29.654	0.499

Note: The value presents as Mean ± SD.

Table 6. Baseline ECG characterization of rs57326399 in BrS patients

Parameters	CC	CT	*P* value
Heart rate (bpm)	74.585 ± 12.970	75.515 ± 12.463	0.717
PR II (ms)	165.931 ± 23.712	162.901 ± 31.480	0.563
PR V2 (ms)	162.283 ± 24.384	158.231 ± 31.567	0.435
QRS II (ms)	100.193 ± 12.570	95.672 ± 13.380	0.083
QRS V2 (ms)	101.020 ± 12.832	98.494 ± 12.638	0.319
QTc II (ms)	404.509 ± 31.887	409.171 ± 30.718	0.474
QTc V2 (ms)	402.584 ± 32.991	409.681 ± 30.940	0.276

Note: The value presents as Mean ± SD.

recovery from inactivation in comparison to A1073. Both of these effects contribute to a loss of function of I_{Na}, accounting for the electrocardiographic differences observed in carriers of V1073.

SCN10A common variant in intron (rs10428132) has been reported to be strongly associated with BrS in one recent GWAS (4,9). And rs6795970 and rs12632942 had a high and moderate linkage disequilibrium with rs10428132 ($r^2 = 0.933$, 0.220) which implied their possible association with BrS (7,18). In addition, a recent association study based on 156 European-descent BrS patients also suggested V1073 has a strong association with BrS, consistent with our findings (11). It is well appreciated that genotype frequencies of common variants vary in different ethnic populations. The cases enrolled in our study derive from European, African and Asian backgrounds. No significant deviation

Table 7. Baseline ECG characterization of rs12632942 in BrS patients

Parameters	GG	AG	*P* value
Heart rate (bpm)	74.083 ± 12.238	77.323 ± 14.579	0.516
PR II (ms)	165.215 ± 24.313	165.162 ± 30.444	0.992
PR V2 (ms)	161.850 ± 25.066	159.392 ± 30.283	0.645
QRS II (ms)	99.696 ± 13.169	97.095 ± 11.723	0.331
QRS V2 (ms)	100.583 ± 13.119	99.795 ± 11.781	0.761
QTc II (ms)	405.357 ± 31.907	406.450 ± 30.845	0.870
QTc V2 (ms)	403.591 ± 33.114	406.662 ± 30.892	0.645

Note: The value presents as Mean ± SD.

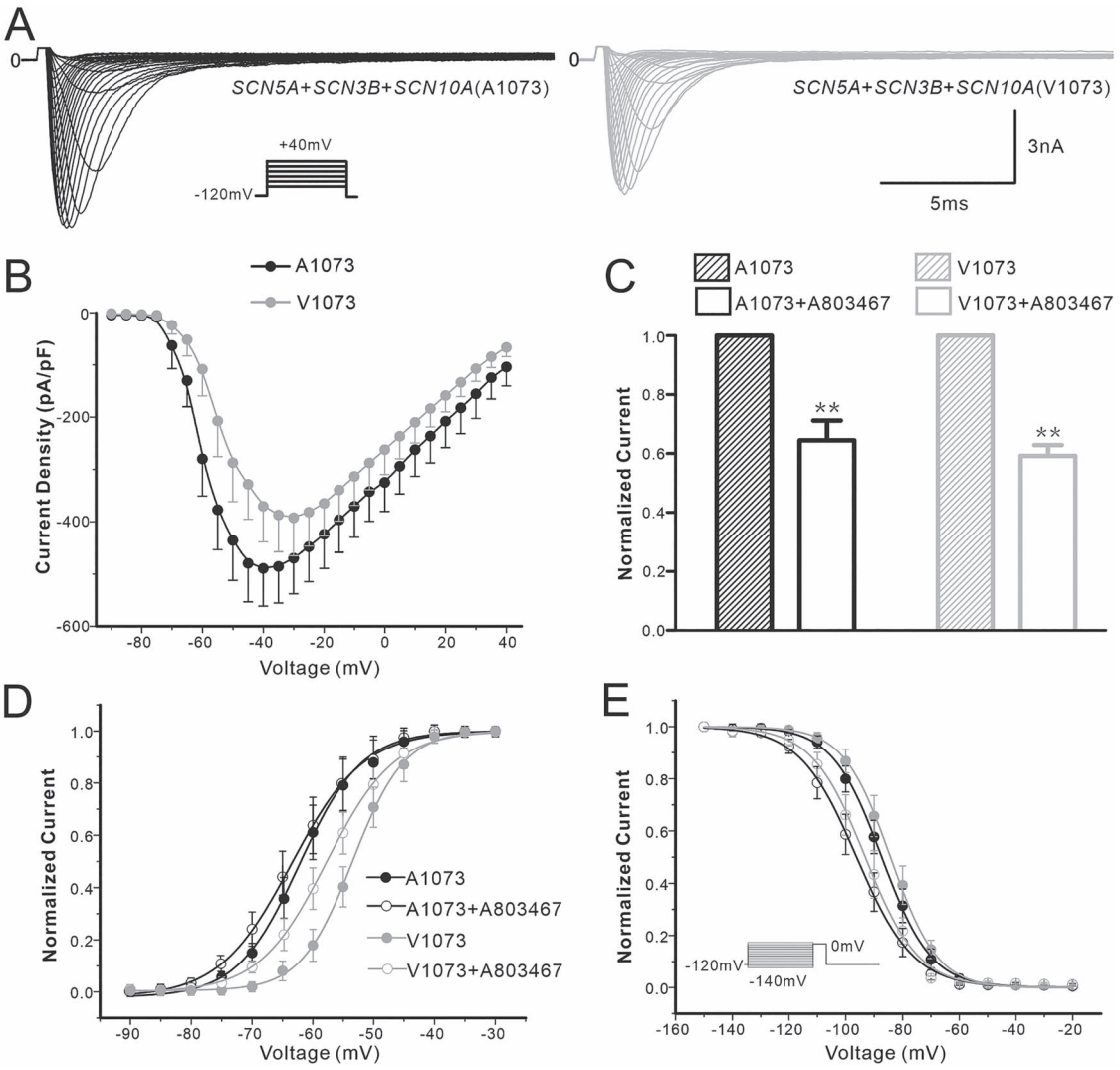

Figure 1. Comparison of current–voltage relationship, steady-state activation and inactivation in *SCN5A–SCN3B–SCN10A* (A1073 or V1073) transfected TSA201 cells in the absence or presence of A-803467. **(A)** Representative $I_{Na,P}$ traces in *SCN5A* + *SCN3B* + SCN10A-A1073 co-transfected cells (black) and *SCN5A* + *SCN3B* + SCN10A-V1073 co-transfected cells (red). **(B)** Current–voltage relationship compared between *SCN5A* + *SCN3B* + SCN10A-A1073 and *SCN5A* + *SCN3B* + SCN10A-V1073 channels. **(C)** Relative blocking effect of 100 nM A-803467 on $I_{Na,P}$ of A1073 and V1073 transfected cells. $^{**}P < 0.01$ compared with the current in the absence of A-803467, $n = 13$ in A1073, $n = 15$ in V1073. **(D)** Steady-state activation in A1073 and V1073 transfected cells before and after the drug. **(E)** Steady-state inactivation in both kinds of transfected cells before and after the drug.

of the 4 BrS-associated common variants was detected in the test of Hardy–Weinberg equilibrium (Supplementary Table S1). An association study performed by Andreasen *et al.* (19) suggested that the BrS risk loci appear to be associated with AF. In their study, rs10428132 played a protective role in AF patients ($OR = 0.73$, $P = 5.7 \times 10^{-6}$). Not surprisingly, G allele (A1073) in rs6795970 has recently been reported to modulate AF risk (8). Genome-wide and phenome-wide analysis by Ritchie *et al.* (20)

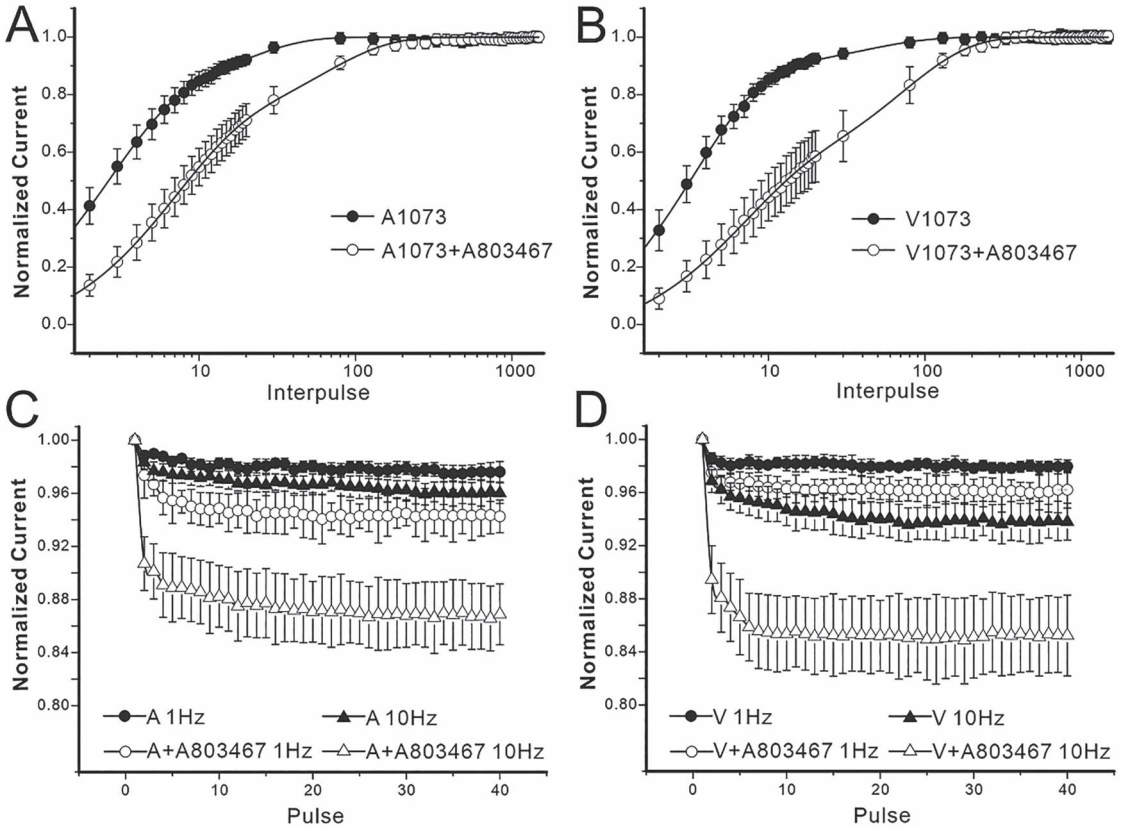

Figure 2. Recovery from inactivation and use-dependent block of *SCN5A–SCN3B–SCN10A* (A1073 or V1073) transfected TSA201 cells before and after A-803467. **(A, B)** Recovery from inactivation of A1073 and V1073 before and after A-803467 at 100 nM fitted by bi-exponential. **(C, D)** Use-dependent block at 1 and 10 Hz on $I_{Na,P}$ of A1073 and V1073 before and after the drug.

determined a direct association of rs6795970 with AF, that carriage of G allele has a lower rate free of AF compared with that of the A allele during follow-up of 5272 originally normal cardiac conduction/normal heart patients. Jabbari *et al.* (8) recruited 225 lone AF and also observed a strong association between rs6795970 and AF (OR = 1.35 for G allele, $P = 2.3 \times 10^{-5}$). Moreover, rs6795970 was also reported to be associated with AF recurrence after catheter ablation (21). In our study, carrying an 'A' allele in this locus leads to a three times higher risk for development to BrS. Additionally, we identified three other common variants associated with BrS whose minor alleles tended to be protective of susceptibility to BrS (Table 3).

Multiple GWAS concluded that rs6795970 is strongly associated with prolonged PR interval and QRS duration, either directly or indirectly by linkage to the sentinel SNP such as rs6800541 and rs6801957 (18,22). ECG from 1192 AF patients by Delaney *et al.* (23) revealed an association with rs6795970 and rs12632942 Both variants were associated with PR interval on unadjusted analysis and only rs6795970 remained after adjustment. However, all three BrS-associated variants identified in our study had no statistically significant association with PR interval, QRS or QTc duration. Similar observations were reported in the study by Behr *et al.* (11). These findings were not withstanding, we observed a trend for V1073 carriers to display a slower HR, wider QRS and shorter QTc interval compared with A1073. These results suggest that more BrS patients may need to be included in the association study with ECG parameters. Ritchie *et al.* (20) suggested that the associations of rs6795970 with QRS duration and cardiac arrhythmias (including AF) were independent. Hence, the susceptibility to BrS resulting from this variant may not be completely reflected in the ECG parameters and a more invasive approach related to BrS risk such as signal average ECG or QT dispersion may be revealing (24,25).

Recent studies have reported comparisons in electrophysiological properties between A1073 and V1073. Both probed the possible effects of rs6795970 on arrhythmias on the basis of *SCN10A* plasmid transfection into neuronal cell lines-ND7/23 or neuro2A cells. But the results were contradictory in the two neuronal cell lines. Inactivation $V_{1/2}$ was very significantly more negative for V1073 than for A1073 in the Behr *et al.* study, pointing to a loss of function due to gating differences, but no difference in the Jabbari study (8,11). In our study, we disclose positive shift in activation and slowed recovery in *SCN10A*-V1073 cells co-transfected with *SCN5A*, which indicates an impaired channel function of the former group.

To what extent Nav1.8 contributes to cardiac electrophysiology and the molecular mechanism(s) involved remain a matter of debate (3,26). The relevance of the *SCN5A–SCN10A* locus to BrS has been reported in a BrS cohort study with 312 patients of European ancestry (9). Van den Boogaard and colleagues demonstrated that a common genetic variant within *SCN10A* modulates cardiac *SCN5A* expression (17).

Because manifestation of a BrS phenotype secondary to a sodium channel loss of function requires reduction of at least 50% of I_{Na} availability (27), it is unlikely that loss of function of the tiny Nav1.8 (*SCN10A*) current, even if it exists within the human heart, is sufficient to result in a BrS phenotype (26). We hypothesized that the most reasonable way for *SCN10A* to

Table 8. Gating kinetics in *SCN5A–SCN3B–SCN10A* co-transfected TSA201 cells before and after A-803467

SCN5A–SCN3B–SCN10A transfected cells	Steady-state activation			Steady-state inactivation			Recovery		
	$V_{1/2}$	K	N	$V_{1/2}$	K	N	τ_{fast}	τ_{slow}	N
A1073 before the drug[a]	−62.202 ± 2.637	5.129 ± 0.328	10	−87.339 ± 2.394	8.659 ± 0.953	18	2.459 ± 0.299	16.661 ± 3.434	17
A1073 after the drug[a]	−63.551 ± 2.674	5.925 ± 0.275*	10	−96.195 ± 2.996*	10.039 ± 1.242	18	6.499 ± 1.67*	60.379 ± 9.532*	17
V1073 before the drug[a]	−53.45 ± 1.566†	4.237 ± 0.358	14	−84.232 ± 2.480	8.252 ± 0.366	15	3.281 ± 0.504	38.473 ± 10.877†	10
V1073 after the drug[a]	−57.723 ± 1.898*	5.552 ± 0.387*	14	−93.157 ± 2.980*	9.363 ± 0.829	15	6.067 ± 2.04*	71.494 ± 12.224*	10

Note: The value presents as Mean ± SEM.
[a]Drug refers to A-803467 at 100 nM.
*$P < 0.05$ before versus after the drug.
†$P < 0.05$ A1073 versus V1073 transfected cells before the drug.

generate a BrS phenotype is by influencing *SCN5A*. Accordingly, we co-expressed *SCN5A–SCN10A* plasmids in TSA201 cells to test this hypothesis and to explore the differences between A1073 and V1073, the two alleles of rs6795970. It is noteworthy that at present there is no evidence for the existence of such a complex in the human heart and that co-immunoprecipitation of the two plasmids, although demonstrated in heterologous expression systems (10), has not been demonstrated using human ventricular cardiomyocytes. Our findings suggest that the combination of a reduced current density (Fig. 1D), dramatic positive shift of steady-state activation (Fig. 1C) and slowing of recovery for inactivation (Fig. 2) of *SCN5A–SCN10A*-V1073 channels can reduce availability of sodium channel current to produce the BrS phenotype. As far as the response to Nav1.8 specific blocker, A-803467 can make the activation more hyperpolarized in V1073 group. It results in less prolongation effect on the recovery from inactivation and less blocking effect on use-dependency in V1073 group, which suggests this Nav1.8 selective drug is losing its dominant power in the variant channel that warrants further study.

Conclusions

In the present study, we enrolled 197 BrS patients and identified four *SCN10A* common variants (rs7630989, rs57326399, rs6795970, rs12632942) that displayed a significant association with BrS susceptibility. There were no evident associations between baseline ECG parameters in BrS patients and the different genotypes of the four variants. Rs6795970 was revealed to be strongly related to the risk of BrS and patients carrying the A allele (V1073) tended to have a slower HR, wider QRS duration and shorter QTc intervals, consistent with the reduced availability of I_{Na} demonstrated for this allele in functional studies. The functional studies were carried out in *SCN5A–SCN10A* co-transfected TSA201 cells. The positive shift in steady-state activation and slowed recovery from inactivation observed in the V1073 cells suggest the impaired function of sodium channel and rs6795970 variant leads to BrS phonotype by influencing *SCN5A*.

Materials and Methods

Patient population and clinical analysis

We studied 197 unrelated BrS probands, referred to our center between May 2008 and May 2020. BrS is diagnosed according to the recent Expert Consensus Statement. (2) All patients included in the study had a type I ST segment elevation (BrS ECG) with ST-segment ≥2 mm in ≥1 lead among the right precordial leads either spontaneously or after provocative drug testing using intravenous administration of sodium channel blockers (ajmaline, flecainide, pilsicainide or procainamide). Patients with electrolyte disturbance at the time of diagnosis or structural heart diseases examined by echocardiography and exercise testing were excluded. Informed consent was obtained from all these patients. The study was approved by the institutional review board at Renmin Hospital of Wuhan University (Wuhan, China) and conducted according to Declaration of Helsinki principles.

Genetic screening

Blood was collected from patients after obtaining informed consent. Genomic DNA was extracted from peripheral blood leukocytes and amplified all exons and intron borders of *SCN10A*.

Amplified samples were sequenced on Ion Torrent Personal Genome Machine (Life Technologies, Carlsbad, CA). Run quality was assessed using the Coverage Analysis plugin to report average depth of coverage, uniformity of coverage, and percent on target as well as other metrics. Uncovered variants were confirmed by Sanger sequencing.

ECG analysis

About 12 leads ECG (25 or 50 mm/s paper speed and 1 cm/mV amplification) of all enrolled patients were obtained. All measurements were performed in a blinded fashion by three experienced trained observers and mean values were calculated and acquired. Baseline ECG was used to measure PR interval, QRS duration, RR interval, HR, QT interval, corrected QT (QTc) (by Bazett's formula, $QTc = QT/RR^{1/2}$) in lead II and V2. AF, early repolarization (ER) pattern and conduction disease (including atrioventricular block, bundle branch block and bifascicular block) were also evaluated.

Co-expression of Nav1.5 and Nav1.8 and patch clamp study

TSA-201 cells transfected with *SCN5A* wild-type (WT), *SCN3B* WT and *SCN10A* plasmids were used for voltage-clamp study as previously described. (26) Briefly, transient transfection using fugene6 (Roche Diagnostics, Indianapolis, Indiana), was carried out with *SCN10A*, *SCN5A* and *SCN3B* with a molar ratio of 5:5:1 (for a total of 2.25 μg of DNA). Further patch-clamp studies were implemented in 48–72 h after transfection.

All recordings were obtained at room temperature using an Axon patch 200B amplifier (Molecular Devices, Union City, California). Currents were filtered at 5 kHz and digitized at 50 kHz. Series resistance was compensated at around 80%. Cells were allowed to stabilize for 10 min after establishment of the whole-cell configuration before current was measured. Bath solution perfusion contained (in mM): 140 NaCl, 4 KCl, 1.8 $CaCl_2$, 1 $MgCl_2$, 10 HEPES, 10 Dextrose (pH 7.35 with NaOH). Patch pipette were pulled using a gravity puller (PP-830, Narishige International USA, Inc., East Meadow, New York) to obtain resistance between 0.8 and 2.2 MΩ, which were fabricated from 1.5 mm OD borosilicate glass capillaries (Fisher Scientific Inc.). They were filled with a pipette solution containing (in mM) 10 NaF, 105 CsF, 20 CsCl, 2 EGTA and 10 HEPES with a pH of 7.35 adjusted with CsOH and an osmolality of 300 mmol/kg with sucrose. Peak sodium channel current ($I_{Na,P}$) was elicited by depolarizing pulses ranging from −90 to +40 mV in 5 mV increments with a holding potential of −120 mV. Steady-state activation and inactivation were fitted by Boltzmann function $I/I_{max} = 1/(1 + \exp((V - V_{1/2})/k))$, determining the membrane potential of the half-maximal activation and inactivation voltage ($V_{1/2}$) and slope factor (K). Pulses for recovery from inactivation were of 100 ms duration for P1 and 50 ms for P2. Peak current elicited during the second pulse was normalized to the value obtained during the initial test pulse. It was fitted by a double exponential function: $I(t)/I_{max} = A_{fast} \bullet (1 - \exp(-t/\tau_{fast})) + A_{slow} \bullet (1 - \exp(-t/\tau_{slow}))$, where A_{fast} and A_{slow} are the fractions of fast and slow inactivating components, respectively, and τ_{fast} and τ_{slow} are their time constants. Data were analyzed by pCLAMP 10 (Molecular Devices, CA, USA) and Origin Pro 9.0 software (OriginLab Corporation, MA, USA).

Statistics

Continuous variables with normal distribution are presented as mean ± standard deviation. Those continuous data between two groups were analyzed by the independent Student's *t* test. Mann–Whitney *U* test and Kruskal–Wallis *H* test were used for nonparametric data. General liner model was applied to compare the differences in the ECG parameters among the three genotypes. Age and gender were used for adjustment. Logistic regression was performed in the analysis of categorical variables. χ^2 test was employed to test the genetic associations between the cases and controls and deviation from the Hardy–Weinberg equilibrium.

Supplementary Material

Supplementary material is available at *HMG* online.

Author Contribution

D.H., Y.H., XM.C. designed the study. Y.H., XM.C., D.H. performed clinical study subjects and basic experiments. H.B.M, H.J., C.A., coordinated the clinical evaluations. D.H., Y.H., XM.C. and H.B.M. analyzed the data. D.H., Y.H. and XM.C. wrote the manuscript. H.B.M., H.J. and C.A. revised the manuscript. All co-authors contributed to critical editing of the manuscript.

Acknowledgements

The authors are grateful to Ryan Pfeiffer from Masonic Medical Research Institute, USA, for technical assistance.

Conflict of Interest Statement: Dr Antzelevitch served as a consultant and received grant funds from Novartis and Trevena Inc. All other authors report no relationships to disclose.

Funding

National Natural Science Foundation of China (No. 81670304), China; the Fundamental Research Funds for the Central Universities of China (No. 2042019kf0058) and the National Institutes of Health of USA (NIH R56 [HL47678], NIH R01 [HL138103], NIH R01 [HL152201]); the W.W. Smith Charitable Trust and the Wistar and Martha Morris Fund.

References

1. Obeyesekere, M.N., Antzelevitch, C. and Krahn, A.D. (2015) Management of ventricular arrhythmias in suspected channelopathies. *Circ. Arrhythm. Electrophysiol.*, **8**, 221–231.
2. Priori, S.G., Wilde, A.A., Horie, M., Cho, Y., Behr, E.R., Berul, C., Blom, N., Brugada, J., Chiang, C.E., Huikuri, H. *et al.* (2013) HRS/EHRA/APHRS expert consensus statement on the diagnosis and management of patients with inherited primary arrhythmia syndromes: document endorsed by HRS, EHRA, and APHRS in may 2013 and by ACCF, AHA, PACES, and AEPC in June 2013. *Heart Rhythm.*, **10**, 1932–1963.
3. Perez-Agustin, A., Pinsach-Abuin, M.L. and Pagans, S. (2020) Role of non-coding variants in Brugada syndrome. *Int. J. Mol. Sci.*, **21**, 8556.
4. Makarawate, P., Glinge, C., Khongphatthanayothin, A., Walsh, R., Mauleekoonphairoj, J., Amnueypol, M., Prechawat, S., Wongcharoen, W., Krittayaphong, R., Anannab, A. *et al.* (2020) Common and rare susceptibility genetic variants predisposing to Brugada syndrome in Thailand. *Heart Rhythm.*, **17**, 2145–2153.

5. Weng, L.C., Hall, A.W., Choi, S.H., Jurgens, S.J., Haessler, J., Bihlmeyer, N.A., Grarup, N., Lin, H., Teumer, A., Li-Gao, R. *et al.* (2020) Genetic determinants of electrocardiographic P-wave duration and relation to atrial fibrillation. *Circ. Genom. Precis. Med.*, **13**, 387–395.
6. van Setten, J., Brody, J.A., Jamshidi, Y., Swenson, B.R., Butler, A.M., Campbell, H., Del Greco, F.M., Evans, D.S., Gibson, Q., Gudbjartsson, D.F. *et al.* (2018) PR interval genome-wide association meta-analysis identifies 50 loci associated with atrial and atrioventricular electrical activity. *Nat. Commun.*, **9**, 2904.
7. Macri, V., Brody, J.A., Arking, D.E., Hucker, W.J., Yin, X., Lin, H., Mills, R.W., Sinner, M.F., Lubitz, S.A., Liu, C.T. *et al.* (2018) Common coding variants in SCN10A are associated with the Nav1.8 late current and cardiac conduction. *Circ. Genom. Precis. Med.*, **11**, e001663.
8. Jabbari, J., Olesen, M.S., Yuan, L., Nielsen, J.B., Liang, B., Macri, V., Christophersen, I.E., Nielsen, N., Sajadieh, A., Ellinor, P.T. *et al.* (2015) Common and rare variants in SCN10A modulate the risk of atrial fibrillation. *Circ. Cardiovasc. Genet.*, **8**, 64–73.
9. Bezzina, C.R., Barc, J., Mizusawa, Y., Remme, C.A., Gourraud, J.B., Simonet, F., Verkerk, A.O., Schwartz, P.J., Crotti, L., Dagradi, F. *et al.* (2013) Common variants at SCN5A-SCN10A and HEY2 are associated with Brugada syndrome, a rare disease with high risk of sudden cardiac death. *Nat. Genet.*, **45**, 1044–1049.
10. Hu, D., Barajas-Martinez, H., Pfeiffer, R., Dezi, F., Pfeiffer, J., Buch, T., Betzenhauser, M.J., Belardinelli, L., Kahlig, K.M., Rajamani, S. *et al.* (2014) Mutations in SCN10A are responsible for a large fraction of cases of Brugada syndrome. *J. Am. Coll. Cardiol.*, **64**, 66–79.
11. Behr, E.R., Savio-Galimberti, E., Barc, J., Holst, A.G., Petropoulou, E., Prins, B.P., Jabbari, J., Torchio, M., Berthet, M., Mizusawa, Y. *et al.* (2015) Role of common and rare variants in SCN10A: results from the Brugada syndrome QRS locus gene discovery collaborative study. *Cardiovasc. Res.*, **106**, 520–529.
12. Fukuyama, M., Ohno, S., Makiyama, T. and Horie, M. (2016) Novel SCN10A variants associated with Brugada syndrome. *Europace*, **18**, 905–911.
13. Yang, T., Atack, T.C., Stroud, D.M., Zhang, W., Hall, L. and Roden, D.M. (2012) Blocking Scn10a channels in heart reduces late sodium current and is antiarrhythmic. *Circ. Res.*, **111**, 322–332.
14. Stroud, D.M., Yang, T., Bersell, K., Kryshtal, D.O., Nagao, S., Shaffer, C., Short, L., Hall, L., Atack, T.C., Zhang, W. *et al.* (2016) Contrasting Nav1.8 activity in Scn10a−/− ventricular myocytes and the intact heart. *J. Am. Heart Assoc.*, **5**, e002946.
15. Gando, I., Williams, N., Fishman, G.I., Sampson, B.A., Tang, Y. and Coetzee, W.A. (2019) Functional characterization of SCN10A variants in several cases of sudden unexplained death. *Forensic Sci. Int.*, **301**, 289–298.
16. van den Boogaard, M., Wong, L.Y., Tessadori, F., Bakker, M.L., Dreizehnter, L.K., Wakker, V., Bezzina, C.R., THoen, P.A., Bakkers, J., Barnett, P. *et al.* (2012) Genetic variation in T-box binding element functionally affects SCN5A/SCN10A enhancer. *J. Clin. Invest.*, **122**, 2519–2530.
17. van den Boogaard, M., Smemo, S., Burnicka-Turek, O., Arnolds, D.E., van de Werken, H.J., Klous, P., McKean, D., Muehlschlegel, J.D., Moosmann, J., Toka, O. *et al.* (2014) A common genetic variant within SCN10A modulates cardiac SCN5A expression. *J. Clin. Invest.*, **124**, 1844–1852.
18. Pfeufer, A., van Noord, C., Marciante, K.D., Arking, D.E., Larson, M.G., Smith, A.V., Tarasov, K.V., Muller, M., Sotoodehnia, N., Sinner, M.F. *et al.* (2010) Genome-wide association study of PR interval. *Nat. Genet.*, **42**, 153–159.
19. Andreasen, L., Nielsen, J.B., Darkner, S., Christophersen, I.E., Jabbari, J., Refsgaard, L., Thiis, J.J., Sajadieh, A., Tveit, A., Haunso, S. *et al.* (2014) Brugada syndrome risk loci seem protective against atrial fibrillation. *Eur. J. Hum. Genet.*, **22**, 1357–1361.
20. Ritchie, M.D., Denny, J.C., Zuvich, R.L., Crawford, D.C., Schildcrout, J.S., Bastarache, L., Ramirez, A.H., Mosley, J.D., Pulley, J.M., Basford, M.A. *et al.* (2013) Genome- and phenome-wide analyses of cardiac conduction identifies markers of arrhythmia risk. *Circulation*, **127**, 1377–1385.
21. Wu, H., Xu, J., Chen, S., Zhou, G., Qi, B., Wei, Y., Hu, E., Tang, D., Chen, G., Li, H. *et al.* (2017) Association of SCN10A polymorphisms with the recurrence of atrial fibrillation after catheter ablation in a Chinese Han population. *Sci. Rep.*, **7**, 44003.
22. Sotoodehnia, N., Isaacs, A., de Bakker, P.I., Dorr, M., Newton-Cheh, C., Nolte, I.M., van der Harst, P., Muller, M., Eijgelsheim, M., Alonso, A. *et al.* (2010) Common variants in 22 loci are associated with QRS duration and cardiac ventricular conduction. *Nat. Genet.*, **42**, 1068–1076.
23. Delaney, J.T., Muhammad, R., Shi, Y., Schildcrout, J.S., Blair, M., Short, L., Roden, D.M. and Darbar, D. (2014) Common SCN10A variants modulate PR interval and heart rate response during atrial fibrillation. *Europace*, **16**, 485–490.
24. Sommariva, E., Pappone, C., Martinelli Boneschi, F., Di Resta, C., Rosaria Carbone, M., Salvi, E., Vergara, P., Sala, S., Cusi, D., Ferrari, M. *et al.* (2013) Genetics can contribute to the prognosis of Brugada syndrome: a pilot model for risk stratification. *Eur. J. Hum. Genet.*, **21**, 911–917.
25. Priori, S.G., Gasparini, M., Napolitano, C., Della Bella, P., Ottonelli, A.G., Sassone, B., Giordano, U., Pappone, C., Mascioli, G., Rossetti, G. *et al.* (2012) Risk stratification in Brugada syndrome: results of the PRELUDE (PRogrammed ELectrical stimUlation preDictive valuE) registry. *J. Am. Coll. Cardiol.*, **59**, 37–45.
26. Chen, X., Yu, L., Shi, S., Jiang, H., Huang, C., Desai, M., Li, Y., Barajas-Martinez, H. and Hu, D. (2016) Neuronal Nav1.8 channels as a novel therapeutic target of acute atrial fibrillation prevention. *J. Am. Heart Assoc.*, **5**, e004050.
27. Sroubek, J., Probst, V., Mazzanti, A., Delise, P., Hevia, J.C., Ohkubo, K., Zorzi, A., Champagne, J., Kostopoulou, A., Yin, X. *et al.* (2016) Programmed ventricular stimulation for risk stratification in the Brugada syndrome: a pooled analysis. *Circulation*, **133**, 622–630.